ResearchGate

See discussions, stats, and author profiles for this publication at: https://www.researchgate.net/publication/231680667

Motions of Water, Decane, and Bis(2-ethylhexyl)sulfosuccinate Sodium Salt in Reverse Micelle Solutions

ARTICLE *in* LANGMUIR · JUNE 1999

Impact Factor: 4.46 · DOI: 10.1021/la9812119

CITATIONS
31

READS
46

5 AUTHORS, INCLUDING:

Joseph Hornak
Rochester Institute of Technology

65 PUBLICATIONS **669** CITATIONS

SEE PROFILE

Available from: Joseph Hornak
Retrieved on: 26 January 2016

Articles

Motions of Water, Decane, and Bis(2-ethylhexyl)sulfosuccinate Sodium Salt in Reverse Micelle Solutions

L. J. Schwartz,[†] C. L. DeCiantis,[†] S. Chapman,[‡] B. K. Kelley,[‡] and J. P. Hornak*[,‡,§]

Department of Chemistry, St. John Fisher College, Rochester, New York 14618, Department of Chemistry, Rochester Institute of Technology, Rochester, New York 14623-5604, and Center for Imaging Science, Rochester Institute of Technology, Rochester, New York 14623-5604

Received September 9, 1998. In Final Form: March 16, 1999

Reverse micellar solutions made from the surfactant bis(2-ethylhexyl)sulfosuccinate sodium salt (AOT), water, and decane have been studied using NMR inversion−recovery and pulsed-field gradient experiments. Spin-lattice relaxation times, T_1, and diffusion coefficients, D, were measured for the individual components of the reverse micellar phase of the water−AOT−decane microemulsion as a function of temperature, 277 < T < 313 K, and reverse micelle volume fraction, 0 < ϕ < 1. Activation energies for the decane rotational motions probed by the T_1 measurements and those for the translational motions probed by the D measurements are compared as a function of ϕ. Both types of activation energies increase by a factor of ∼2 as ϕ increases from zero (pure decane) to 0.8 (near the lamellar phase boundary), indicating the influence of the AOT tails on the decane motions. A $T-\phi$ phase diagram has been constructed showing an empirical boundary for the onset of percolation. This percolation characterization, together with the measured diffusion coefficients and relaxation times, is consistent with previous descriptions of the structure and dynamics of water−AOT−decane and similar microemulsions reported in the literature. This study also continues the evaluation of the water−AOT−decane microemulsion as the signal-bearing solution in a magnetic resonance imaging phantom. The T_1 of the water phase matches that of nonfatty tissues in the body; however, the hydrocarbon component will need to be adjusted to match its T_1 to that of adipose tissue. The percolation boundary in the $T-\phi$ phase diagram helps to define the T and ϕ values where the solution possesses the high dielectric constant needed to minimize a standing wave artifact in a magnetic resonance image of the phantom.

Introduction

Reverse micellar solutions made from the surfactant bis(2-ethylhexyl)sulfosuccinate sodium salt (AOT), water, and decane have been proposed for use in phantoms to test and calibrate the performance of magnetic resonance imagers.[1] These solutions possess nuclear magnetic resonance (NMR) chemical shift components and radio-frequency electrical properties that are similar to those of tissues in the human body. A preliminary study of the overall proton spin−lattice and spin−spin relaxation parameters, T_1 and T_2, for this system has been reported.[2] This work showed that the overall proton T_1 and T_2 values can be adjusted by the addition of paramagnetic salts to the aqueous phase. The proton T_1 values of the solutions were found to display very little dependence on temperature, T, but did depend strongly on volume fraction, ϕ, defined as

$$\phi = \frac{V_{\mathrm{AOT}} + V_{\mathrm{H_2O}}}{V_{\mathrm{AOT}} + V_{\mathrm{H_2O}} + V_{\mathrm{Decane}}} \quad (1)$$

where V_i is the volume of component i. These results are intriguing but ambiguous because the T_1 values represent an approximation to the weighted-average relaxation times of the total solution. A clearer picture will be possible if the T_1 values of the individual water and decane signals are obtained separately. The question also still remained as to whether the T_1 values of the individual water and decane signals are close to those of muscle and adipose tissues, respectively. This is an important property because it allows a phantom solution imaged at room temperature to respond to imaging sequences in a manner similar to that of the human body (37 °C). In order to resolve these issues, a detailed study of the T_1 values of the individual water and decane components of the same reverse micelle solutions, as a function of temperature and ϕ, has been undertaken.

In addition to characterizing this system in terms of its potential as a phantom, NMR relaxation studies can also be used to obtain information on both its structure and motional characteristics, as shown by previous studies of micellar systems.[3−6] Rotational correlation times are most directly obtained from ^{2}H and ^{17}O NMR studies; the

* To whom correspondence should be addressed. E-mail: jphsch@rit.edu. Fax: 716 475-5988. Tel: 716 475-2904.
[†] St. John Fisher College.
[‡] Department of Chemistry, Rochester Institute of Technology.
[§] Center for Imaging Science, Rochester Institute of Technology.

(1) Roe, J. E.; Prentice, W. E.; Hornak, J. P. *Magn. Reson. Med*. **1996**, *35*, 136.
(2) Roe, J. E.; Ramanan, D. D.; Hornak, J. P.; Kotlarchyk, M. *Phys. A* **1996**, *231*, 359.
(3) Carlström, G.; Halle, B. *J. Phys. Chem*. **1989**, *93*, 3287.

10.1021/la9812119 CCC: $18.00 © 1999 American Chemical Society
Published on Web 06/18/1999

relaxation of these two isotopes is due to intramolecular quadrupolar coupling, leading to T_1 relaxation rates which reflect the rotational motion of individual molecules. In contrast, ^{1}H relaxes via both intramolecular and intermolecular dipole−dipole interactions, and its T_1 relaxation rate therefore does not reflect only the motion of individual molecules.[7] In addition, it is difficult to extract the rotational correlation time because it depends on the specific motional model that is assumed. For the purposes of this paper, T_1 will be considered as an empirical parameter which gives a snapshot of the rotational motions present at the Larmor frequency.

Another metric of molecular motions is the translational diffusion coefficient, D. The magnitude of a translational diffusion coefficient can be directly related to the root-mean-square distance, $\langle z^2\rangle^{1/2}$, traveled by the species during a given time, t:

$$\langle z^2\rangle^{1/2} = (2Dt)^{1/2} \quad (2)$$

Pulsed-field gradient NMR[8−10] (also known as pulsed-gradient spin-echo [PGSE] NMR) and light scattering[11−13] techniques have been used to obtain translational diffusion coefficients for a wide variety of systems, including water−AOT−decane microemulsions.[14−17] Not only do pulsed-field gradient NMR diffusion measurements report on entirely different motions than do T_1 measurements (translations vs rotations) but also the two techniques sample motions on entirely different time scales (milliseconds vs nanoseconds).

Feldman et al.[15] have studied the temperature dependence of the diffusion coefficients of the individual components of a water−AOT−decane microemulsion having $\phi = 0.39$ and reverse micelle diameters of approximately 75 Å. Their goal was to characterize the temperature dependence of the onset of percolation for that system, a phenomenon whereby the reverse micelles merge and form channels through which the water can travel.[16−20] Percolation can decrease the dielectric constant of a microemulsion,[15] rendering it less useful as a solution for use in a magnetic resonance imaging phantom. For example, a phantom solution with a low dielectric constant can create a standing wave artifact in its image.[1] Therefore, knowledge of the percolation threshold as a function of ϕ for a micellar solution proposed as a phantom would also be helpful in choosing an appropriate ϕ.

The present paper complements and extends the Feldman et al.[15] study by measuring the diffusion coefficients of the water, AOT, and decane components of a series of micellar solutions described in detail below, as a function of both T and ϕ. The results have been used to construct a $T-\phi$ phase diagram that shows the percolation threshold of the system. The percolation characterization, together with the measured diffusion coefficients and T_1 values, helps to create a simple picture of the structure and dynamics of the water−AOT−decane microemulsion.

Experimental Section

Microemulsions were prepared in the range $0.95 \geq \phi \geq 0.05$ in steps of 0.05 ± 0.01, using AOT (Fluka Chemika, >98%), water (J.T. Baker Analyzed HPLC reagent), $NiCl_2$ (Fisher Scientific, >99%), and *n*-decane (Fluka Chemika, >95%). The chemicals were used as received from the manufacturers, without further purification. The mass ratio of water to AOT was held constant at 1.65 (mole ratio = 40.8). This mass ratio results in reverse micelles with average diameters of roughly 100 Å.[21]

The water phase was doped with $NiCl_2$ to a concentration of 8 mM (approximately 0.1 wt %) to keep the experimental conditions the same as those in the previous study.[2] At this level of doping, there are on average 5 Ni^{2+} ions and 500 Na^+ ions (from the AOT molecules) per reverse micelle. The addition of such a low concentration of $NiCl_2$ to the ionic environment already present is not expected to grossly alter either the phase boundary or the droplet microstructure of the reverse micelle phase. (Reports of such changes with added salt are based on a concentration of 0.6 wt %.[16,17,19]) While the paramagnetic Ni^{2+} ions will affect the water T_1 values, they should not affect the water diffusion coefficients.

All measurements were done on a 7.05 T (300 MHz) Bruker Avance spectrometer equipped with a maximum *z*-field gradient of 0.55 T/m. Because of the broad spectral line widths (full width at half-height values on the order of 10 Hz), the spectrometer could be run unlocked; periodic shimming was done on a sample identical to the $\phi = 0.50$ microemulsion except for the replacement of H_2O by D_2O. The 5 mm NMR tubes were spun for the T_1 measurements but not for the diffusion measurements.

Spin−lattice relaxation times and diffusion coefficients were measured at 277, 283, 294, 303, and 313 K. The solutions were equilibrated in a water bath before they were used, and only solutions which showed a single, clear phase were used. The phase boundaries found in this study were consistent with earlier work.[2,21] In the spectrometer, the temperature of the samples was controlled using a Bruker BV 3300 Eurotherm temperature controller. The temperature variation was ±0.1 K for all temperatures except 294 K, where the variation was ±1 K. The temperatures are accurate to ±1 K (measured using a methanol NMR thermometer).[22]

T_1 values were obtained using an inversion-recovery sequence with 16 averages and a 10 s repetition delay time. After Fourier transformation of the free induction decay (FID), monoexponential nonlinear least-squares fits were applied to integrals taken over the water, decane CH_2, and decane CH_3 peak regions. No points were omitted in the fits.

Diffusion coefficients were measured using the stimulated-echo pulsed-field gradient diffusion sequence[8,23] having bipolar pulse pairs and a longitudinal eddy current delay.[24] The amplitude of the FID signal that occurs after the fifth 90° pulse is a sum of contributions from each proton making up the components in solution. The signal attenuation, E_i, due to the diffusion of each of the protons is given by

(4) Yoshino, A.; Yoshida, T.; Takahashi, K.; Ueda, I. *J. Colloid Interface Sci.* **1989**, *133*, 390.
(5) Yoshino, A.; Okabayashi, H.; Yoshida, T. *J. Phys. Chem.* **1994**, *98*, 7036.
(6) Lindman, B.; Olsson, U. *Ber. Bunsen-Ges. Phys. Chem.* **1996**, *100*, 344.
(7) Carper, W. R.; Keller, C. E. *J. Phys. Chem. A* **1997**, *101*, 3246.
(8) Stilbs, P. *Prog. NMR Spectrosc.* **1987**, *19*, 1.
(9) Price, W. S. *Concepts Magn. Reson.* **1997**, *9*, 299.
(10) Price, W. S. *Concepts Magn. Reson.* **1998**, *10*, 197.
(11) Berne, B. J.; Pecora, R. *Dynamic Light Scattering*; Wiley: New York, 1976.
(12) Rondelez, F.; Hervet, H.; Urback, W. *Chem. Phys. Lett.* **1978**, *53*, 138.
(13) Wesson, J. A.; Takezoe, H.; Yu, H.; Chen, S. P. *J. Appl. Phys.* **1982**, *53*, 6513.
(14) Kim, M. W.; Dozier, W. D. In *Micellar Solutions and Microemulsions*; Chen, S. H., Rajagopalan, R., Eds.; Springer-Verlag: New York, 1991; p 291.
(15) Feldman, Y.; Kozlovich, N.; Nir, I.; Garti, N.; Archipov, V.; Idiyatullin, Z.; Zuev, Y.; Fedotov, V. *J. Phys. Chem.* **1996**, *100*, 3745.
(16) Texter, J.; Antalek, B.; Williams, A. J. *J. Chem. Phys.* **1997**, *106*, 7869.
(17) Antalek, B.; Williams, A. J.; Texter, J.; Feldman, Y.; Garti, N. *Colloids Surf. A* **1997**, *128*, 1.
(18) Hamilton, R. T.; Billman, J. F.; Kaler, E. W. *Langmuir* **1990**, *6*, 1696.
(19) Chen, S.-H.; Chang, S.-L.; Strey, R. *J. Chem. Phys.* **1990**, *93*, 1907.
(20) Antalek, B.; Williams, A. J.; Texter, J. *J. Phys. Rev. E* **1996**, *54*, R5913.
(21) Kotlarchyk, M.; Sheu, E. Y.; Capel, M. *Phys. Rev. A* **1992**, *46*, 928.
(22) Raiford, D. S.; Fisk, C. L.; Becker, E. D. *Anal. Chem.* **1979**, *51*, 2050.
(23) Tanner, J. E. *J. Chem. Phys.* **1970**, *52*, 2523.
(24) Wu, D.; Chen, A.; Johnson, C. S., Jr. *J. Magn. Reson., Series A* **1995**, *115*, 260.

$$E_i = \exp[-\gamma^2 D_i g^2 \delta^2 (\Delta - \delta/3 - \tau_g/2)] \quad (3)$$

where γ is the gyromagnetic ratio, D_i is the diffusion coefficient of the ith proton, g is the strength of the magnetic field gradient, $\delta/2$ is the width of the individual gradient pulses, Δ is the time between the leading edges of the two positive gradient pulses, and τ_g is the time between the trailing edge of each negative gradient pulse and the next 90° pulse.[10] The experiments were run as a function of g; gradients from 0.011 to 0.484 T/m were used, while Δ, δ, and τ_g were kept constant at 0.306, 0.002, and 0.002 s, respectively. The repetition delay between scans was 10 s. The diffusion parameters were chosen to be optimal for the overlapped decane and AOT tail proton region of the NMR spectrum (approximately 1.5−0.5 ppm). Plots of $\ln(A_i)$ vs g^2 from this region showed biexponential behavior, with a decrease of at least an order of magnitude, reflecting the diffusion of both the decane protons and the slower moving AOT tail protons.

Diffusion coefficients were obtained for protons on the water molecules, on the decane molecules, near the headgroup of the AOT molecules, and on the tail of the AOT molecules. Diffusion coefficients for the AOT tail protons and for the decane molecules were obtained by applying a biexponential fit[25] to the integrals taken over the overlapped decane and AOT tail proton region. Diffusion coefficients for the AOT head protons and for the water molecules were obtained by applying a linear least-squares fit to integrals taken over the AOT and water peaks with approximate values of 4.1−3.6 and 4.7−4.2 ppm, respectively.

Results and Discussion

Spin−Lattice Relaxation Time. Figure 1 shows the T_1 values of the decane CH_3 protons and the Ni^{2+}-doped water protons as a function of T and ϕ. The T_1 values of the CH_2 protons (not shown) are very similar to those of the CH_3 protons. This similarity implies that, at the Larmor frequency (300 MHz), the density of molecular motions that affect the T_1 of the decane CH_2 protons is similar to the density of motions that affect the T_1 of the decane CH_3 protons. The T_1 values of the decane CH_3 protons decrease as ϕ increases. Thus, at the Larmor frequency, the density of motions that affect the T_1 of the decane molecules increases as the reverse micelle volume fraction increases.

The decane CH_3 T_1 values increase as the temperature increases. The activation energy, E_A, of the motions probed by the T_1 measurements is obtained by plotting $\ln(1/T_1)$ vs $1/T$ and is shown in Figure 2 as a function of ϕ. The activation energy of pure decane is 10.0 ± 0.4 kJ/mol, and the activation energy of the decane in the reverse micelle phase increases nonlinearly with ϕ until it is roughly double that value at $\phi = 0.8$.

The ϕ-dependent activation energy can be rationalized by assuming that the decane molecules are in two pools: a bulk phase and a phase that is in close association with the tails of the AOT molecule. A fast exchange of decane molecules between these two pools would result in a single T_1 value being measured, which would reflect the weighted average of the T_1 relaxation times of the respective pools. As the volume fraction of reverse micelles increases, the relative numbers of decane molecules in the two pools will change accordingly, along with the weighted average of the T_1 relaxation times. Thus, in this model, the nature of the interaction between the decane molecules and the tails of the AOT molecules remains constant as ϕ changes, and it is only the changing relative sizes of the two pools which explains the change in the T_1 relaxation times as a function of ϕ.

(25) A four-parameter gradient expansion algorithm implemented in IDL, Interactive Data Language, V5.0, Research Systems, Inc., Boulder, CO.

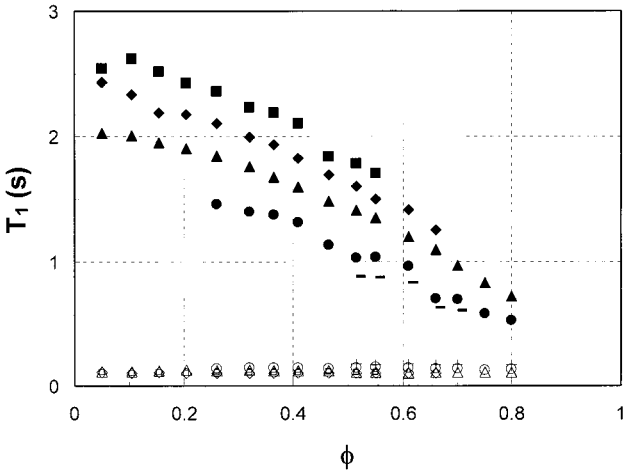

Figure 1. Proton T_1 values at 300 MHz for the decane CH_3 and H_2O hydrogens in the water−AOT−decane microemulsions as a function of ϕ. Decane: 277 (−), 283 (●), 294 (▲), 303 (◆), and 313 (■) K. Water: 277 (+), 283 (○), 294 (△), 303 (◇), and 313 (□) K.

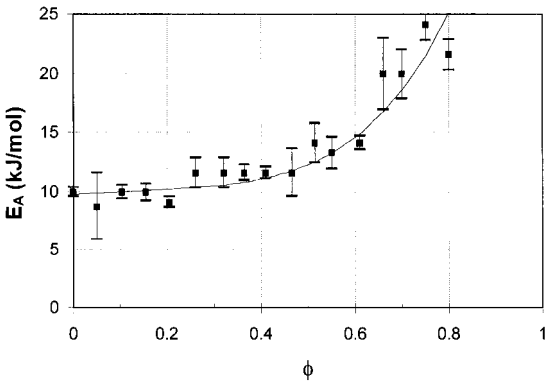

Figure 2. Activation energy for the decane rotational motions responsible for the decane T_1 at 300 MHz, in the water−AOT−decane microemulsions as a function of ϕ. The solid line is drawn to guide the eye.

Table 1. Comparison of T_1 (s) Values for Aqueous 8 mM $NiCl_2$

T (K)	bulk	reverse micelle
277	0.16	0.17
283	0.14	0.14
294	0.11	0.12
303	0.12	0.10
313	0.15	0.11

In contrast to the T_1 values of decane, the T_1 values of doped water have an additional contribution from the modulation of the electron−nuclear dipolar interaction[26−28] by electron spin flips of the paramagnetic Ni^{2+}. Table 1 compares the T_1 values of the doped water in the reverse micellar phase, averaged over all ϕ values, to those in bulk solutions of 8 mM $NiCl_2$. The similarity of the two sets of data in Table 1 suggests that the effect of the Ni^{2+} ions on the water molecules in the reverse micelles is the same as that on water molecules in bulk water and that, in the reverse micelle solutions, the interaction with the paramagnetic Ni^{2+} is the dominant mechanism for the water proton relaxation. The small divergence at higher

(26) Friedman, H. L.; Holz, M.; Hertz, H. G. *J. Chem. Phys.* **1979**, *70*, 3369.
(27) Kraft, K. A.; Fatouros, P. P.; Clarke, G. D.; Kishore, P. R. S. *Magn. Reson. Med.* **1987**, *5*, 555.
(28) Glasel, J. A. In *Water: A Comprehensive Treatise*; Franks, F., Ed.; Plenum Press: New York, 1972; Vol. 1, p 215.

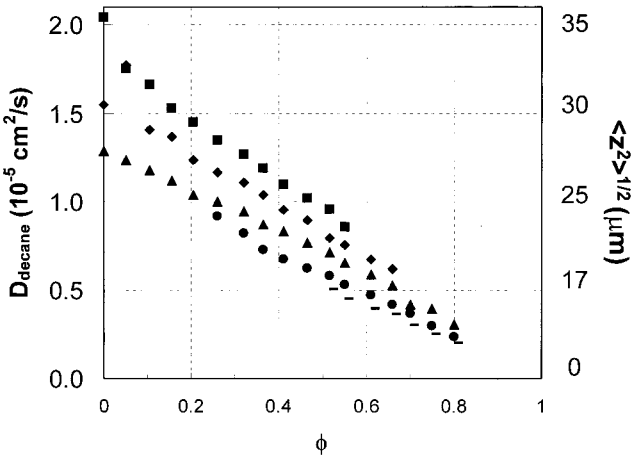

Figure 3. D and $\langle z^2 \rangle^{1/2}$ for decane in the water−AOT−decane microemulsions as a function of ϕ for $T = 277$ (-), 283 (●), 294 (▲), 303 (◆), and 313 (■) K.

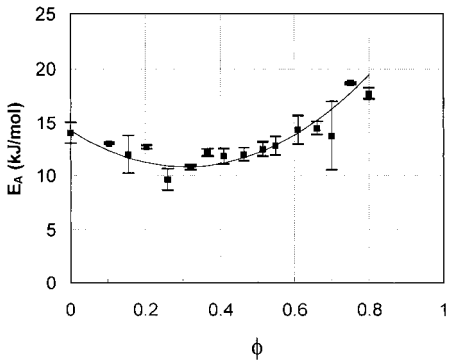

Figure 4. Activation energy for the decane translational motion in the water−AOT−decane microemulsions as a function of ϕ. The solid line is drawn to guide the eye.

temperatures indicates that some other relaxation mechanism may be playing an additional role.

The finding that T_1 values of doped water have a much weaker dependence on ϕ and T than T_1 values of decane (see Figure 1) can thus be explained by the domination of the water relaxation by the interactions with Ni^{2+} and possibly also by the assumption that any deformation of the micelles due to changes in ϕ does not strongly influence the density of the motions that affect T_1.

Diffusion. Figure 3 presents the diffusion coefficients of the decane molecules as a function of ϕ and T. The decane molecules have a larger diffusion coefficient and are thus able to move further away, on average, from a given starting position, as the temperature increases and/or the reverse micelle volume fraction decreases. The root-mean-square distance traveled by the decane molecules from the beginning of the first pair of gradient pulses to the beginning of the second pair of gradient pulses ($\Delta = 0.306$ s) ranges from ∼10 to 30 μm or from ∼1000 to 3000 average micelle diameters.

The activation energy of translation of the decane molecules (which can be thought of as the minimum energy needed for a decane molecule to break out of a cage of its nearest neighbors) is obtained by plotting ln(D) as a function of $1/T$. A linear relationship was found for each ϕ value, and the resulting activation energies are shown in Figure 4 as a function of ϕ. The translational activation energy of pure decane is 14 ± 1 kJ/mol. The data suggest a slight decrease in E_A as a function of ϕ, before a stronger increase to a value of ∼20 kJ/mol at $\phi = 0.8$. Compared to the activation energy of the motions probed by the T_1 measurements, E_A for translation has a slightly less pronounced ϕ dependence. As with the T_1 activation energies, the ϕ dependence reflects the differing degree to which the decane molecules interact with the tails of the AOT molecules as ϕ changes.

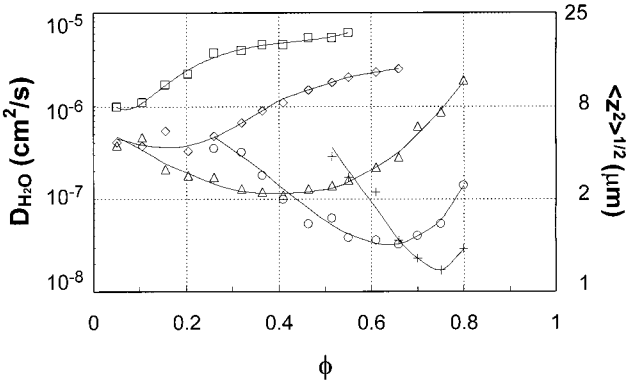

Figure 5. D and $\langle z^2 \rangle^{1/2}$ for water in the water−AOT−decane microemulsions as a function of ϕ for $T = 277$ (+), 283 (○), 294 (△), 303 (◇), and 313 (□) K.

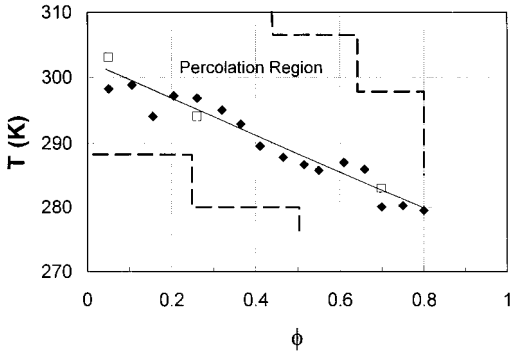

Figure 6. $T-\phi$ percolation boundary in the reverse micelle phase, as indicated by the temperatures at which the H_2O diffusion coefficients have their minimum values (◆), and the minimum ϕ values at which the AOT and H_2O diffusion coefficients diverge from each other (□). See text for details. The solid line is drawn to guide the eye. The dashed lines mark the approximate boundaries of the reverse micelle phase.

Figure 5 shows the diffusion coefficients of the H_2O molecules as a function of ϕ, for each of the temperatures studied. The diffusion coefficients have been plotted on a log scale to highlight the similar ϕ dependence of the curves even though they vary over 3 orders of magnitude. The diffusion coefficients appear to first decrease, and then increase, as a function of ϕ. The higher the temperature, the lower the ϕ at which the minimum in the diffusion coefficient curve occurs; at the highest temperature, only the rise with increasing ϕ values is seen. As will be discussed further below, these minima are assumed to reflect the onset of percolation. In order to get a rough idea of the temperature at which each solution of a given ϕ has its minimum diffusion coefficient, the data were also plotted as a function of temperature (not shown) and fit with polynomial functions. Figure 6 shows the temperatures at which the minimum H_2O diffusion coefficients occur using ◆ symbols. Consistent with Figure 5, the higher the ϕ value, the lower the temperature at which the minimum H_2O diffusion coefficient occurs. Figure 6 can be interpreted as a phase diagram which shows the boundary in the $T-\phi$ domain which separates the conditions where the system exists as intact reverse micelles from those where the system has begun to show signs of percolation.

Figure 7 plots the decane and H_2O diffusion coefficients

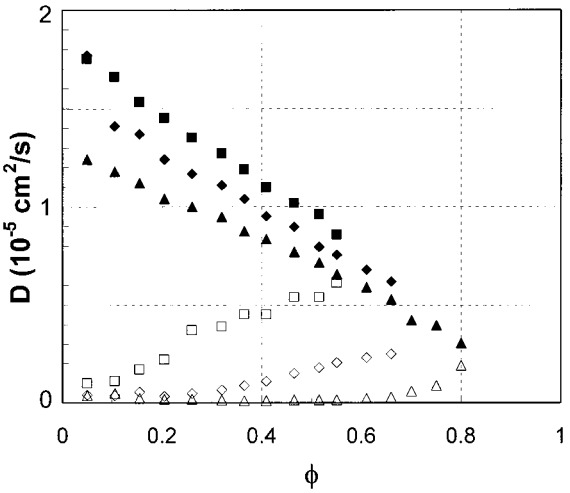

Figure 7. *D* for decane and water in the water-AOT-microemulsions as a function of ϕ. Decane: 294 (▲), 303 (◆), and 313 (■) K. Water: 294 (△), 303 (◇), and 313 (□) K.

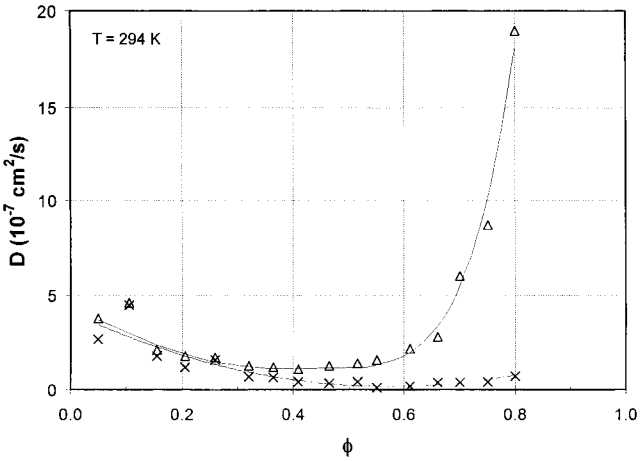

Figure 8. *D* for water and AOT head group protons in the water−AOT−decane microemulsions at 294 K. Water: (△). AOT: (×). Lines are drawn to guide the eye.

for the three highest temperatures on the same graph. The trends for the lower two temperatures are consistent but less pronounced. The figure shows how the decane and H_2O diffusion coefficients approach each other as the state of the system approaches the phase boundary.

The AOT head and tail diffusion coefficients both decrease and then generally level off as ϕ increases. Figure 8 compares the diffusion coefficients of the water and the AOT head group protons at 294 K. (Results at the other temperatures, and for the AOT tail region protons, are consistent but not shown.) At low ϕ, the diffusion coefficients of the water and the AOT head group protons are similar; however, at the ϕ value where the diffusion coefficients of the water molecules begin to increase, those of the head group of the AOT molecules remain constant.

The ϕ value at which the D_{AOT} and D_{H_2O} curves diverge at each temperature was taken as a second indication of the onset of percolation. Values could be obtained for three of the temperatures studied; they are included as □ symbols in the plot in Figure 6, along with the values derived from the minimum water diffusion coefficients.

A physical picture emerges which is consistent with that of previous studies.[15,17] At low ϕ values, the reverse micelles act independently. Independent reverse micelle motion implies two types of water motion: restricted motions of the individual water molecules within the reverse micelles and coherent group motion of all of the water molecules within a reverse micelle as the reverse micelle diffuses through the decane.

As ϕ increases, the observed H_2O diffusion coefficients decrease. There was no evidence[8,9] found to suggest that the water motion being monitored is the restricted motion of the water within the reverse micelles. First, the magnitudes of the water diffusion coefficients imply that the H_2O molecules have traveled more than 1000 reverse micelle diameters over the course of the experiment (~300 ms). Second, given the large Δ values used and the possible size of any restricting boundaries, it is likely that the effects of restricted diffusion would be well averaged on this time scale. Third, natural log plots of eq 3 always gave straight lines for the water data. Fourth, in this same regime, the diffusion coefficients of the AOT and H_2O molecules track each other. These results imply that the H_2O and AOT diffusion coefficients reflect the translational motion of entire reverse micelles in this regime.

The initial decrease in the water diffusion coefficient as ϕ increases parallels the decrease in the decane diffusion coefficient. Both diffusion coefficients decrease because of the increasing viscosity of the solution, which is caused by the increasingly frequent interactions of the reverse micelles. The minimum in the H_2O diffusion coefficient curves would be expected to occur just before the onset of percolation. When percolation occurs, the reverse micelles merge and channels form. These channels allow for freer H_2O translational motion and hence an increase in the H_2O diffusion coefficient as ϕ continues to increase. For these ϕ values, the H_2O diffusion coefficients reflect the translational motion of individual water molecules. The AOT diffusion coefficients stay fairly constant as ϕ continues to increase, however, because they reflect the much slower movement of the AOT molecules, which are now making up the percolated structure. Near the phase boundary at $\phi > 0.80$, the H_2O and decane diffusion coefficients tend toward the same magnitude. One explanation is that the motion of the two different molecules is becoming equally free in the newly emerging lamellar phase.[21] However, near the phase boundary, the system is quite heterogeneous and the molecular environments for the decane and water molecules are very different. Given the system heterogeneity, it is difficult to claim that both molecules are experiencing the same degree of physical confinement. Therefore, the fact that the diffusion coefficients appear to converge at $\phi \approx 0.80$ may be fortuitous.

Conclusions

This paper has presented measured proton T_1 relaxation times and diffusion coefficients for the components of the water−AOT−decane microemulsion system as a function of T and ϕ. The data have been used to construct a picture of the reverse micelle phase, based on the rotational and translational motions of the decane, water, and AOT molecules, which is consistent with the literature.

The activation energies for the rotational motions probed by T_1 and the translational motions probed by D indicate an increase in the activation barrier in decane for both motions as ϕ increases. These observations support a picture of a decreasing free volume for the decane and more interaction with the AOT tails as ϕ increases. The close match between D_{water}, $D_{AOT-tail}$, and $D_{AOT-head}$ at low ϕ values indicates the presence of distinct reverse micelles. The decrease in D_{water}, $D_{AOT-tail}$, and $D_{AOT-head}$ as ϕ increases through low values indicates a slowing of the reverse micelles and is the result of the increasing effective

viscosity of the reverse micelle solution as the concentration of decane decreases. The divergence of D_{water} from $D_{AOT-tail}$ and $D_{AOT-head}$ as ϕ increases further is supportive of percolation and an increased mean free path for the water to diffuse through. A $T-\phi$ phase diagram has been constructed which shows the boundary for the percolation threshold of the reverse micelles.

This study has also resulted in several specific implications for the use of the system as a phantom in magnetic resonance imagers. The $T-\phi$ phase diagram indicates that a ϕ value below about 0.3 should be used in order to construct a phantom from these solutions which is free from percolation at room temperature. The T_1 data show that Ni^{2+} affects the water molecules in the reverse micelles the same way that it affects bulk water and that the water T_1 is comparable to that of the nonfatty tissues in the human body. However, the magnitudes of the T_1 values of decane are not similar to those of the adipose tissue in the body.[29] Therefore, an aliphatic paramagnetic relaxation agent would need to be added to the decane to reduce its T_1 value to that of adipose tissue.

Acknowledgment. We thank St. John Fisher College for funding the sabbatical leave for L.J.S. and NSF REU CHE-9424025 for sponsoring S.C. and C.L.D. We also thank B. Antalek, S. Kennedy, M. Kotlarchyk, W. Maas, and C. Sotak for helpful discussions.

LA9812119

(29) Fletcher, L. M.; Barsotti, J. B.; Hornak, J. P. *Magn. Reson. Med.* **1993**, *29*, 623.